

## The precession of orbital plane and the significant variabilities of binary pulsars

Bipeng Gong

Department of Astronomy, Nanjing University, Nanjing 210093, P.R. China

bpgong@nju.edu.cn

## ABSTRACT

There are two kinds of expressions on the precession of orbital plane of a binary pulsar system. This paper analyzes that one expression is inconsistent with the conservation of the total angular momentum vector; whereas the other one is consistent with it. And the reason is that the former is obtained in the case of 12 degree of freedom to a binary pulsar system is; whereas the other one corresponds to 9 degree of freedom. Calculating the spin-orbit coupling induced effects of a binary pulsar system under 9 degree of freedom, significant variabilities to binary parameters can be obtained, which can interpret the observations of three typical binary pulsars, PSR J2051-0827, PSR J1012+5307, and PSR J1713+0747. The situation is similar to the calculation of the motion of a small mass at the bottom of a clock pendulum. If we assume that the degree of freedom of this small mass is 2, then this small mass can move every in the 2-dimension space, and the length of the pendulum is not a constant. On the other hand once the length of the pendulum is a constant, the degree of freedom is 1 instead of 2. And calculating under 2 or 1 degree of freedom corresponds to different predictions on the motion of a small mass at the bottom of a clock pendulum.

**Subject headings:** pulsars: binary pulsars, geodetic precession

## 1. Introduction

In the gravitational two-body problem with spin, each body is precessing in the gravitational field of its companion, with precession velocity of 1 Post-Newtonian order (PN) by Barker & O'Connell (1975), hereafter BO. This precession velocity is widely accepted. But how does the orbital plane react to the torque caused by the precession of the two bodies has two kinds of treatments. BO's orbital precession velocity is obtained by assuming that the angular momentum vector,  $\mathbf{L}$ , precesses at the same velocity as the Runge-Lenz vector,  $\mathbf{A}$ .

On the other hand, in the study of the modulation of the gravitational wave by SL coupling effect on merging binaries (Apostolatos et al. (1994), Kidder (1995), hereafter AK) obtain an orbital precession velocity that satisfies the conservation of the total angular momentum,  $\mathbf{J}$ , and

the triangle constraint,  $J = L + S$  (where  $S$  is the sum of spin angular momenta of two bodies,  $S_1$  and  $S_2$ ).

The discrepancy in the assumptions leads to different behaviors in physics between BO and AK's orbital precession velocities. The former cannot be consistent with the triangle constraint, whereas the latter can. And the reason of this discrepancy is that the former assumes that the four vectors,  $S_1$ ,  $S_2$ ,  $r_1$  and  $r_2$  ( $r_1$ ,  $r_2$  are position vectors of the two bodies respectively), are independent, and the degree of freedom of the binary system is 12; whereas, the latter actually assumes that the independent vectors are either  $S_1$ ,  $r_1$  and  $r_2$ ; or  $S_2$ ,  $r_1$  and  $r_2$ . And the degree of freedom is 9.

The discrepancy between the two different precession velocities is similar to the following case. The motion of a small mass at the bottom of a clock pendulum can be described in  $x$ – $y$  plane. However if we say that the degree of freedom of this small mass is 2, then this small mass can move every in the 2-dimension space, and the length of the pendulum is not a constant. In other words, once the length of the pendulum is a constant, the degree of freedom is 1 instead of 2. Correspondingly if the degree of freedom of a binary system is 12, as treated by BO, then the triangle constraint cannot be satisfied (or  $J$  cannot be a constant vector). On the other hand, if the triangle constraint is satisfied, the degree of freedom cannot be 12, instead it is 9.

In the application to pulsar timing measurement, the predicted effect of this paper can explain not only the first derivative of the projected semimajor axes,  $\dot{x}$ , but also  $x$ ,  $P_b$ , and  $P_b$  of three typical binary pulsars, PSR J2051-0827, PSR J1012+5307, and PSR J1713+0747.

The arrangement is as follows: Sec 2 introduces the derivation of orbital precession velocity of BO and AK. Sec 3 analyzes that the difference between BO and AK is physical, one violates the conservation of  $J$  and one satisfies it. And why BO's orbital precession velocity violates the conservation of  $J$  is analyzed.

In Sect 4, the equation of motion of a binary system is obtained in the case that  $J = L + S$  is satisfied and the degree of freedom is 9, from which the S-L coupling induced orbital precession velocity and advance of precession of periastron are obtained through perturbation method in celestial mechanics. Sect 5 derives variabilities caused by the S-L coupling induced effect. Sect 6 applies the new model to three typical binary pulsars, and explains the significant variabilities that cannot be well interpreted by former models. Sect 7 concludes that whether  $J = L + S$  is satisfied or not, can cause very different predictions on the binary parameters of a binary pulsar system, although all derivations start from the same point, general relativity. Sect 8 is the appendix, giving the perturbation of other four orbital elements.

## 2. orbital precession velocity

This section introduces the derivation of the orbital precession velocity of BO and AK.

### 2.1. Derivation of BO's orbital precession velocity

BO's two-body equation was the first gravitational two-body equation with spin, which consists of two parts, the precession velocity of the spin angular momentum vectors of body one and body two, and the precession velocity of the orbital angular momentum vector.

Body one precesses in the gravitational field of body two, with precession velocity of BO,

$$\dot{\mathbf{L}}_1 = \frac{L(4 + 3m_2 - m_1)}{2r^3} \hat{\mathbf{L}} + \frac{S_2}{2r^3} \hat{\mathbf{S}}_2 - 3(\hat{\mathbf{L}} \cdot \hat{\mathbf{S}}_2) \hat{\mathbf{L}}^i \quad (1)$$

where  $\hat{\mathbf{L}}$ ,  $\hat{\mathbf{S}}_1$  and  $\hat{\mathbf{S}}_2$  are unit vectors of the orbital angular momentum, the spin angular momentum of star 1 and star 2, respectively.

$\dot{\mathbf{L}}_2$  can be obtained by exchanging the subscript 1 and 2 at the right side of Eq.(1). The first term of Eq.(1) represents the geodetic (de Sitter) precession, which corresponds to the precession of  $S_1$  around  $L$ , it is 1PN due to  $\frac{L}{r^3} \left(\frac{v}{c}\right)^2 \left(\frac{v}{c}\right)$ ; and the second term represents the Lense-Thirring precession,  $S_1$  around  $S_2$ , which is  $\frac{S}{L}$  times smaller than the first, therefore, it corresponds to 1.5PN. The precession velocity of the spin angular momentum vectors is computed by other authors using different methods.

However for the precession velocity of the orbit, there are different expressions. BO's orbital precession velocity is given as follows.

The total Hamiltonian for the gravitational two-body problem with spin is given (BO, Damour & Schaefer (1988)),

$$H = H_N + H_{1PN} + H_{2PN} + H_S; \quad (2)$$

where  $H_N$ ,  $H_{1PN}$  and  $H_{2PN}$  are the Newtonian, the first and second order post-Newtonian terms respectively.  $H_S$  is the spin-orbit interaction Hamiltonian (BO, Damour & Schaefer (1988)),

$$H_S = \sum_{m=1}^{\infty} \left(2 + 3\frac{m+1}{m}\right) \left(\frac{S}{r^3}\right) L; \quad (3)$$

where  $+1$  is meant modulo 2 ( $2+1=1$ ),  $m_1, m_2$  are the masses of the two stars, respectively,  $r = a(1 - e^2)^{1/2}$ ,  $a$  is the semi-major axis,  $e$  is the eccentricity of the orbit. Notice we use  $G = c = 1$  until discussing observational effects in Sec 5 and Sec 6.

The BO equation describes the secular effect of the orbital plane by a rotational velocity vector,  $\dot{\mathbf{L}}$ , acting on some instantaneous Newtonian ellipse. Damour & Schaefer (1988) computed  $\dot{\mathbf{L}}$  in a simple manner by making full use of the Hamiltonian method.

The functions of the canonically conjugate phase space variables  $r$  and  $p$  are defined as

$$L(r;p) = r - p; \quad (4)$$

$$A(r;p) = p - L - GM^2 \frac{r}{r}; \quad (5)$$

where  $r = r_1 + r_2$ ,  $M = m_1 + m_2$ ,  $\mathbf{A} = m_1 m_2 \mathbf{M}$ . The vector  $\mathbf{A}$  is the Runge-Lenz vector (first discovered by Lagrange). The instantaneous Newtonian ellipse evolves according to the fundamental equations of Hamiltonian dynamics (Damour & Schäfer (1988))

$$\dot{\mathbf{L}} = f\mathbf{L}; \mathbf{H} \mathbf{g}; \quad (6)$$

$$\dot{\mathbf{A}} = f\mathbf{A}; \mathbf{H} \mathbf{g}; \quad (7)$$

where  $f;g$  denote the Poisson bracket.  $\mathbf{L}$  and  $\mathbf{A}$  are first integrals of  $\mathbf{H}_N$ , only  $\mathbf{H}_{1PN} + \mathbf{H}_{2PN} + \mathbf{H}_S$  contributes to the right-hand sides of Eq.(6) and Eq.(7), in which  $\mathbf{H}_{1PN} + \mathbf{H}_{2PN}$  determines the precession of periastron, in 1PN it is given,

$$\dot{\mathbf{L}}^{GR} = \frac{6M}{P_b a(1-\epsilon^2)}; \quad (8)$$

where  $P_b$  is the orbital period. To study the spin-orbit interaction, it is sufficient to consider  $\mathbf{H}_S$ . Thus replacing  $\mathbf{H}$  of Eq.(6) and Eq.(7) by  $\mathbf{H}_S$  obtains (Damour & Schäfer (1988)),

$$(\frac{d\mathbf{L}}{dt})_S = f\mathbf{L}; \mathbf{H}_S \mathbf{g} = -_S \hat{\mathbf{S}} \cdot \mathbf{L}; \quad (9)$$

$$(\frac{d\mathbf{A}}{dt})_S = f\mathbf{A}; \mathbf{H}_S \mathbf{g} = -_S \hat{\mathbf{S}} \cdot [3\hat{\mathbf{L}} \cdot \hat{\mathbf{S}}] \hat{\mathbf{L}} \cdot \mathbf{A}; \quad (10)$$

where

$$-_S = \frac{S(4 + 3m_2 - m_1)}{2r^3}; \quad (11)$$

By Damour & Schäfer ((1988)),  $\mathbf{S}$  represents a linear combination of  $\mathbf{S}_1$  and  $\mathbf{S}_2$ . For simplicity of discussion, and for consistency with Wex & Kopeikin ((1999))'s application of  $-_S$ , we assume  $\mathbf{S} = \mathbf{S}_1$  (the other spin angular momentum is ignored) until Sec 4 where the general binary pulsar is discussed.

The solution of Eq.(9) and Eq.(10) gives the  $\mathbf{S}$ - $\mathbf{L}$  coupling induced orbital precession velocity (Damour & Schäfer (1988))

$$-_S = -_S \hat{\mathbf{S}} \cdot [3\hat{\mathbf{L}} \cdot \hat{\mathbf{S}}] \hat{\mathbf{L}}; \quad (12)$$

By Eq.(9) and Eq.(12), the first derivative of  $\hat{\mathbf{L}}$  can be obtained,

$$\frac{d\hat{\mathbf{L}}}{dt} = -_S \hat{\mathbf{S}} \cdot \hat{\mathbf{L}}; \quad (13)$$

and by Eq.(1) the first derivative of  $\hat{\mathbf{S}}$  (recall  $\mathbf{S} = \mathbf{S}_1$ ) can be written

$$\frac{d\hat{\mathbf{S}}}{dt} = -_1 \hat{\mathbf{L}} \cdot \hat{\mathbf{S}} = -_S \frac{L}{S} \hat{\mathbf{L}} \cdot \hat{\mathbf{S}}; \quad (14)$$

where  $-_1$  is the first term at the right hand side of Eq.(1). By Eq.(13) and Eq.(14)  $\hat{\mathbf{L}}$  precesses slowly around  $\hat{\mathbf{S}}$ , 1.5PN, as shown by Eq.(13); whereas  $\hat{\mathbf{S}}$  precesses rapidly around  $\hat{\mathbf{L}}$ , 1PN, as shown in Eq.(14). Therefore the BO equation predicts such a scenario that the two vectors,  $\hat{\mathbf{L}}$  and  $\hat{\mathbf{S}}$  precess around each with very different precession velocities (typically one is larger than the other by 3 to 4 orders of magnitude for a general binary pulsar system).

## 2.2. Orbital precession velocity in the calculation of gravitational waves

In the study of the modulation of precession of orbital plane to gravitational waves, the orbital precession velocity is obtained in a different manner and the result is very different from that given by Eq.(12).

Since the gravitational wave corresponding to 2.5PN, which is negligible compared with S-L coupling effect that corresponds to 1PN and 1.5PN, the total angular momentum can be treated as conserved,  $J = 0$ . Then the following equation can be obtained (BO),

$$-0 \quad L = -1 \quad S_1 \quad -2 \quad S_2 : \quad (15)$$

Notice that as defined by BO and AK,  $L = M^{1/2} r^{1/2} \hat{L}$ . In the one-spin case the right hand side of Eq.(15) can be given (Küller (1995)),

$$S = \frac{1}{2r^3} (4 + \frac{3m_2}{m_1}) (L - S); \quad (16)$$

and considering that  $J = L + S$ , Eq.(16) can be written,

$$S = \frac{1}{2r^3} (4 + \frac{3m_2}{m_1}) (J - S) : \quad (17)$$

From Eq.(15),  $L$  can be given,

$$L = \frac{1}{2r^3} (4 + \frac{3m_2}{m_1}) (J - L) : \quad (18)$$

By Eq.(17) and Eq.(18),  $L$  and  $S$  precess about the fixed vector  $J$  at the same rate with a precession frequency approximately (AK)

$$-0 = \frac{J}{2r^3} (4 + \frac{3m_2}{m_1}) : \quad (19)$$

Eq.(19) indicates that in the 1 PN approximation,  $\hat{L}$  and  $\hat{S}$  can precess around  $J$  rapidly (1PN) with exactly the same velocity. Notice that the misalignment angles between  $\hat{L}$  and  $\hat{S}$  ( $\theta_{LS}$ ),  $\hat{L}$  and  $\hat{J}$  ( $\theta_{LJ}$ ) are very different, due to  $S=L=1$ ,  $\theta_{LJ}$  is much smaller than  $\theta_{LS}$ .

Thus, AK's equations, Eq.(18) and Eq.(17), correspond to a very different scenario of motion of  $S$ ,  $L$  and  $J$  from that given by BO equation shown in Eq.(13) and Eq.(14).

## 3. Physical differences between BO and AK

This section compares two different scenarios corresponding to BO and AK's orbital precession velocity, and points out that BO's orbital precession velocity actually violates the definition of the total angular momentum of a binary system.

Section 2 indicates that BO and AK derived the orbital precession velocity in different ways, therefore two different orbital precession velocity vectors are obtained, as shown in Eq.(12) and

Eq.(19), respectively, which in turn correspond to different scenarios of motion of the three vectors. This section points out that the discrepancy between BO and AK is not just a discrepancy corresponding to different coordinate systems. Actually there is significant physical differences between BO and AK. The total angular momentum of a binary system is defined as BO

$$J = L + S ; \quad (20)$$

Eq.(20) means that  $J$ ,  $L$  and  $S$  form a triangle, and therefore, it guarantees that the three vectors must be in one plane at any moment. For a general radio binary pulsar system, the total angular momentum of this system is conserved in 1PN order. Therefore we have

$$J = 0 : \quad (21)$$

Eq.(21) means that  $J$  is a constant during the motion of a binary system. Eq.(21) and Eq.(20) together provide a scenario that the triangle formed by  $L$ ,  $S$  and  $J$  determines a plane, and the plane rotates around a fixed axis,  $J$ , with velocity  $-v_0$ . This scenario is shown in Fig 1. which can also be represented as

$$J = -v_0 \hat{J} \quad L + -v_0 \hat{J} \quad S = 0 ; \quad (22)$$

Smart & Blandford ((1976)) mentioned the scenario that  $L$  and  $S$  must be at opposite side of  $J$  at any instant. Hamilton and Sarazin ((1982)) also study the scenario and state that  $L$  precesses rapidly around  $J$ . Obviously the orbital precession velocity given by Eq.(19) can satisfy the two constraints, Eq.(20) and Eq.(21) simultaneously.

Can the BO's orbital precession velocity given by Eq.(12) satisfy the two constraints, Eq.(20) and Eq.(21) simultaneously? From Eq.(12), Eq.(13) and Eq.(14), the first derivative of  $J$  can be written (BO)

$$J = -v_S \quad L + -v_L \quad S = -v_S \hat{S} \quad L + -v_L \hat{L} \quad S = 0 ; \quad (23)$$

and since Eq.(20) is defined in BO's equation, then it seems that the BO equation can satisfy both Eq.(20) and Eq.(21).

But in BO's derivation of  $-v_S$  (Eq.(6) {Eq.(12)}), Eq.(20) is never used. The corresponding  $-v_S$  can make  $J = L + S = 0$ , as shown in Eq.(23), however it cannot guarantee that  $J = L + S$  is satisfied. In other words, when  $J \neq L + S$ , Eq.(23) is still correct. This can be easily tested by putting  $L^0 = L + S$ , or  $S^0 = S + L$  (and are arbitrary constants) into Eq.(23) to replace  $L$  and  $S$ , respectively, obviously in such cases, Eq.(23) is still satisfied ( $J = 0$ ).

Contrarily in AK's derivation of  $-v_0$  (Eq.(16) {Eq.(18)}), the relation Eq.(20) is used. And if we do the same replacement of  $L^0 = L + S$ , or  $S^0 = S + L$  in Eq.(22), then Eq.(22) is violated ( $J \neq 0$ ). This means that for AK's  $-v_0$ , if Eq.(20) is violated then Eq.(21) is violated also. Thus in AK's expression, the conservation of the total angular momentum is dependent on Eq.(20), whereas, in BO's expression, the conservation of the total angular momentum is independent of Eq.(20). If we rewrite Eq.(20) as,

$$J = L + S + C ; \quad (24)$$

then in BO's expression, the conservation of the total angular momentum can be satisfied in the case that  $C \neq 0$  in Eq.(24); whereas, in AK's expression, the conservation of the total angular momentum is satisfied only when  $C = 0$  in Eq.(24). This means that the discrepancy between BO and AK's orbital precession velocity is physical. It is not just different expression in different coordinate systems or relative to different directions.

Moreover Eq.(22) and Eq.(19) correspond to the following orbital precession velocity,

$$\mathbf{\dot{r}}_0 = -\mathbf{\hat{S}} + \frac{\mathbf{L}}{S} \mathbf{\hat{L}} : \quad (25)$$

Obviously Eq.(25) is not consistent with BO's Eq.(12), which demands that the coefficient of the component along  $\mathbf{\hat{L}}$  be  $= 3\mathbf{\hat{L}} \cdot \mathbf{\hat{S}}$ , instead of  $= \frac{\mathbf{L}}{S}$  as given by Eq.(25).

In other words, once Eq.(20) is satisfied, BO's orbital precession velocity of Eq.(12) must be violated. Therefore, BO's orbital precession velocity cannot be consistent with BO's definition,  $\mathbf{J} = \mathbf{L} + \mathbf{S}$ .

Actually Eq.(25) can be consistent with Eq.(9), however it is contradictory to Eq.(10). The reason of introducing Eq.(10) is that without it, Eq.(9) alone cannot determine a unique solution.

Whereas, Eq.(22) and Eq.(19) can be regarded as solving this problem by using Eq.(9) and Eq.(20) instead of Eq.(9) and Eq.(10) to obtain the orbital precession velocity.

As defined in Eq.(4) and Eq.(5),  $\mathbf{L}$  and  $\mathbf{A}$  are vectors that are determined by different elements in celestial mechanics,  $\mathbf{L}(\cdot; i)$  and  $\mathbf{A}(\cdot; i; \cdot; e)$  respectively. And these two vectors satisfy different physical constraints, i.e.,  $\mathbf{L}$  satisfies Eq.(20) and Eq.(21), whereas,  $\mathbf{A}$  doesn't satisfy these two constraints.

Therefore, it is conceivable that  $\mathbf{L}$  and  $\mathbf{A}$  should correspond to different precession velocities, as given by Eq.(9) and Eq.(10), respectively. However since the discrepancy is only in the  $\mathbf{\hat{L}}$  component, which does not influence the satisfaction of the conservation equation, Eq.(23), thus the discrepancy seems unimportant. And therefore, the precession velocity of  $\mathbf{L}$  is treated equivalently to that of  $\mathbf{A}$ 's, thus the components in  $\mathbf{\hat{L}}$  are both treated as  $= 3\mathbf{\hat{L}} \cdot \mathbf{\hat{S}}$ . Whereas, as given by Eq.(25),  $\mathbf{\hat{L}}$  component must be  $= \frac{\mathbf{L}}{S}$  if the triangle constraint is to be satisfied. Therefore, the violation of the triangle constraint is inevitable under the assumption that  $\mathbf{L}$  and  $\mathbf{A}$  precess at the same velocity.

#### 4. S-L coupling induced effects derived under different degree of freedom

As analyzed in Section 2 and Section 3, whether the triangle constraint is satisfied or not results discrepancy in the orbital precession velocity. This section further analyzes that it is the discrepancy in degree of freedom used by BO and AK that leads to the violation or satisfaction of the triangle constraint.

Since S-L coupling induced orbital precession velocity is just one of the S-L coupling induced effects, to discuss the S-L coupling induced effects on observational parameters, one need to obtain the variation of the six orbital elements under S-L coupling.

The way of doing this is from the Hamiltonian (corresponding to S-L coupling) to equation of motion, and then through perturbation methods in celestial mechanics to obtain S-L coupling induced effects to a observer on the Earth. In this section this process is performed in the case that the degree of freedom of a binary system (with two spins) is 9, in which the triangle constraint is satisfied.

It is convenient to study the motion of a binary system in such a coordinate system (J-coordinate system), in which the total angular momentum,  $J$  is along the z-axes and the invariance plane is in the x-y plane. The J-coordinate system has two advantages.

(a) Once a binary pulsar system is given, the misalignment angle between  $J$  and  $L$ ,  $\omega_{JL}$  is determined, from which  $\omega_s$  (or  $\omega$ ) and  $\omega_s$  (or  $\omega_L$ ) can be obtained easily in the J-coordinate system, which are intrinsic to a binary pulsar system.

(b) Moreover, the J-coordinate system is static relative to the line of sight (after counting out the proper motion). Therefore transforming parameters obtained in the J-coordinates system to observer's coordinate system, S-L coupling induced effects can be obtained reliably.

From Eq.(3), the S-L coupling induced  $H_s$  contains potential part only, therefore we have  $H_s = U$ , where

$$U = U_1 + U_2 = \frac{1}{r^3} (2S + \frac{3m_2}{2m_1} S_1 + \frac{3m_1}{2m_2} S_2) \cdot L ; \quad (26)$$

which can be written as

$$U = \frac{1}{r^3} ({}_1S \cdot L + {}_2S_2 \cdot L) ; \quad (27)$$

where

$${}_1 = {}_2 + \frac{3m_2}{2m_1} ; \quad {}_2 = {}_2 + \frac{3}{2} \left( \frac{m_1}{m_2} - \frac{m_2}{m_1} \right) ; \quad (28)$$

The acceleration is given by

$$a_{so} = -r U = -{}_1 r \frac{(S - L)}{r^3} - {}_2 r \frac{(S_2 - L)}{r^3} ; \quad (29)$$

where,  $r$  represents gradient. In the first term at the right hand side of Eq.(29),  $S$  is given by  $S = S_1 + S_2$ , which is determined by  $S_1^{(i)}$  and  $S_2^{(i)}$  ( $i = 1, 2, 3$ ). And  $L$  is dependent of  $r$  (recall  $r = r_1 - r_2$  and  $r_1^{(i)}, r_2^{(i)}$ ,  $i = 1, 2, 3$  are positions of the two body respectively).

Thus the independent variables of Eq.(29) seem  $3 + 3 = 12$ . However, by the triangle constraint and the conservation of  $J$  given by Eq.(20) and Eq.(21), we have  $J = L + S = L + S_1 + S_2 = \text{const}$  vector, which means that  $S$  and  $L$  are dependent, in other words, these 12 variables are not independent in 1PN approximation.

If we directly calculate Eq.(29) by 12 independent variables then  $J = \text{constant vector}$  must be violated, which is like calculating the motion of a clock pendulum by 2 independent variables, from which the length of the pendulum must be variable, in other words, the constraint that  $\text{length} = \text{constant}$  must be violated in a clock pendulum.

A simple treatment can guarantee that  $J = \text{constant vector}$  be satisfied. That is replacing  $S$  in the equation of motion of Eq.(29) by  $J - L$ . Thus the independent variables can either be  $S_2^{(i)}, r_1^{(i)}$  and  $r_2^{(i)}$ ; or  $S_1^{(i)}, r_1^{(i)}$  and  $r_2^{(i)}$  by different  ${}_1$  and  ${}_2$  from Eq.(27) and Eq.(28), in which the degree of freedom is 9 instead of 12. Thus Eq.(29) can be rewritten

$$r \frac{(S - L)}{r^3} = r \frac{[(J - L) - L]}{r^3} = r \frac{(J - L)}{r^3} - r \frac{(L - L)}{r^3} : \quad (30)$$

where

$$r \frac{(J - L)}{r^3} = \frac{3(L - J)r}{r^5} - \frac{3(J - r)V - r}{r^5} + 2 \frac{(J - V)}{r^3} \quad (31)$$

$$r \frac{(L - L)}{r^3} = \frac{3(L - L)r}{r^5} - \frac{3(L - r)V - r}{r^5} + \frac{(L - V)}{r^3} \quad (32)$$

Notice that the coefficient of the third term at the right hand side of Eq.(31) and Eq.(32) are different, the reason is that  $J$  is not a function of  $r$ , whereas  $L$  is. Put Eq.(31) and Eq.(32) into Eq.(30) and finally into Eq.(29), we have,

$$\begin{aligned} a_{so} = & \frac{3}{r^3} [ {}_1(J - L) \hat{n}(-V) + {}_2(S_2) \hat{n}(-V) ] \\ & + \frac{1}{r^3} [ {}_1(V - J) + {}_1(V - (J - L)) + {}_2(V - S_2) ] \\ & + \frac{3(V - \hat{n})}{r^3} [ {}_1((J - L) \hat{n}) + {}_2(S_2 \hat{n}) ] : \end{aligned} \quad (33)$$

And replacing  $J - L$  by  $S$ , Eq.(33) can be written,

$$\begin{aligned} a_{so} = & \frac{3}{r^3} [ {}_1(S) \hat{n}(-V) + {}_2(S_2) \hat{n}(-V) ] \\ & + \frac{1}{r^3} [ {}_1(V - J) + {}_1(V - S) + {}_2(V - S_2) ] \\ & + \frac{3(V - \hat{n})}{r^3} [ {}_1(S \hat{n}) + {}_2(S_2 \hat{n}) ] : \end{aligned} \quad (34)$$

Obviously all terms at the right hand side of Eq.(34) are 1.5PN except the term containing  $J$ , which is caused by the triangle constraint given by Eq.(30) {Eq.(32)}. If one calculates  $a_{so}$  directly by Eq.(29) without imposing the triangle constraint, then the corresponding result can be given by replacing  $J$  of Eq.(34) by  $S$ ,

$$\begin{aligned} a_{so}^0 = & \frac{3}{r^3} [ {}_1(S) \hat{n}(-V) + {}_2(S_2) \hat{n}(-V) ] \\ & + \frac{2}{r^3} [ {}_1(V - S) + {}_2(V - S_2) ] \end{aligned}$$

{ 10 }

$$+ \frac{3(V \cdot \hat{n})}{r^3} [ \mathbf{S}_1 \cdot \hat{n} + \mathbf{S}_2 \cdot \hat{n} ] : \quad (35)$$

Notice that Eq.(35) is equivalent to the sum of Eq.(52) and Eq.(53) given by the BO equation. The difference between Eq.(34) and Eq.(35) indicates that whether the triangle constraint is satisfied or not (9 or 12 degree of freedom) can lead to significant differences in  $a_{so}$ , which in turn results in significant differences on the predictions of observational effects as discussed in the next section.

Having  $a_{so}$ , we can use the standard method in celestial mechanics to calculate,

$$\hat{S} = a_{so} \hat{n}; \quad \hat{T} = a_{so} \hat{t}; \quad \hat{W} = a_{so} \hat{L}; \quad (36)$$

from which one can calculate the derivative of the six orbit elements and then transform to the observer's coordinate system to compare with observation. In Eq.(34) and Eq.(36)  $\hat{n}$  is the unit vector of  $r$ , which is given by,

$$\hat{n} = P \cos f + Q \sin f; \quad (37)$$

and  $\hat{t}$  is the unit vector that is perpendicular to  $\hat{n}$ ,

$$\hat{t} = P \sin f + Q \cos f; \quad (38)$$

and  $V = p =$ , is given by

$$V = \frac{h}{p} P \cos f + \frac{h}{p} Q (e + \cos f); \quad (39)$$

where  $f$  is the true anomaly,  $p$  is the semi latus rectum,  $p = a(1 - e^2)$ , and  $h$  is the integral of area,  $h = r^2 f$ .  $P$  is given by three components,

$$\begin{aligned} P_x &= \cos \cos! \sin \sin! \cos_{LJ}; \\ P_y &= \sin \cos! + \cos \sin! \cos_{LJ}; \\ P_z &= \sin! \sin_{LJ}; \end{aligned} \quad (40)$$

and  $Q$  is given by three components,

$$\begin{aligned} Q_x &= \cos \sin! \sin \cos! \cos_{LJ}; \\ Q_y &= \sin \sin! + \cos \cos! \cos_{LJ}; \\ Q_z &= \cos! \sin_{LJ}; \end{aligned} \quad (41)$$

The unit vector of  $\hat{L}$  and  $\hat{S}$  ( $= 1, 2$ ) are given,

$$\hat{L} = (\sin_{LJ} \cos_L; \sin_{LJ} \sin_L; \cos_{LJ})^T; \quad (42)$$

$$\hat{S} = (\sin_{JS} \cos_S; \sin_{JS} \sin_S; \cos_{JS})^T; \quad (43)$$

In the perturbation equation, the acceleration of Eq.(34),  $a_{so}$ , is expressed along  $\hat{n}$ ,  $\hat{t}$  and  $\hat{L}$  respectively. We can use  $a_1$ ,  $a_2$  and  $a_3$  to represent terms corresponding to the three brackets [ ] at the right hand side of Eq.(34), respectively. Projecting  $a_1$  onto  $\hat{L}$ , we have

$$W_1 = a_1 \cdot \hat{L} = \frac{3}{r^3} [S_x(n_y V_z - n_z V_y) + S_y(n_z V_x - n_x V_z) + S_z(n_x V_y - n_y V_z)] \\ (n_x \sin \omega_J \cos \iota + n_y \sin \omega_J \sin \iota + n_z \cos \omega_J) \quad (44)$$

where  $n_x$ ,  $n_y$ ,  $n_z$  and  $V_x$ ,  $V_y$ ,  $V_z$  are components of  $\hat{n}$  and  $V$  along axes,  $x$ ,  $y$  and  $z$ , respectively. Similarly, projecting  $a_2$  onto  $\hat{L}$ , we have,

$$W_2 = a_2 \cdot \hat{L} = \frac{1}{r^3} (V_y J \sin \omega_J \cos \iota - V_x J \sin \omega_J \sin \iota) \\ + [\frac{1}{r^3} (V_x S_y - V_y S_x) + \frac{2}{r^3} (V_x S_{2y} - V_y S_{2x})] \cos \omega_J \quad (45)$$

Finally  $a_3$  can also be projected onto  $\hat{L}$ ,

$$W_3 = a_3 \cdot \hat{L} = \frac{\cos \omega_J}{r^3} [{}_1(V_y^r S_x - V_x^r S_y) + {}_2(V_y^r S_{2x} - V_x^r S_{2y})] \quad (46)$$

where  $V_x^r = 3rn_x$ ,  $V_y^r = 3rn_y$  and  $\underline{r} = \frac{eh}{p} \sin f$ . Therefore, the sum of  $W$  is

$$\bar{W} = W_1 + W_2 + W_3 \quad (47)$$

The effect around  $J$  can be obtained by perturbation equations (Roy (1991); Yi (1993); Liu (1993)) and Eq.(47)

$$\frac{d}{dt} = \frac{\bar{W} r \sin(\iota + f)}{na^2} \frac{1}{1 - \epsilon^2} \frac{1}{\sin \omega_J} ; \quad (48)$$

where  $n$  is the angular velocity. Averaging over one orbital period we have

$$\langle \frac{d}{dt} \rangle = \frac{3 \cos \omega_J}{2a^3 (1 - \epsilon^2)^{3/2} \sin \omega_J} (P_z \sin \iota + Q_x \cos \iota) [(P_y Q_z - P_z Q_y) (S_{x-1} + S_{2x-2}) \\ + (P_z Q_x - P_x Q_z) (S_{y-1} + S_{2y-2}) + (P_x Q_y - P_y Q_x) (S_{z-1} + S_{2z-2})] : \quad (49)$$

Notice that the average value of Eq.(49) depends only on  $W_1$ , the contribution of  $W_2$  and  $W_3$  to it is zero. With  $S = \sin \omega_J \quad L$ , we have  $d = dt \quad 3L = 2a^3$ , which corresponds to 1PN.

The  $d\iota/dt$  can be obtained by calculation of  $\mathcal{S} = a_{so} \cdot \hat{n}$  and  $\mathcal{P} = a_{so} \cdot \hat{t}$ . Since  $a_1 \cdot \hat{n}$ ,  $a_1 \cdot \hat{t}$ ,  $a_3 \cdot \hat{n}$  and  $a_3 \cdot \hat{t}$  are 1.5PN, which are negligible in the discussion of 1PN; therefore, it is sufficient to consider the projection of  $a_2$  onto  $\hat{n}$ ,  $\hat{t}$  respectively. And since only the first term of  $a_2$ , as shown in Eq.(29), is 1PN, the other two terms are 1.5PN, which are negligible in the discussion of 1PN, thus we have,

$$\langle (a_2 \cdot \hat{n}) \cos f \rangle = \frac{1}{2} \frac{J}{(1 - \epsilon^2)^{3/2} a^3} \frac{eh}{p} (P_x Q_y - P_y Q_x) ; \quad (50)$$

$$\langle (a_2 \hat{t}) \sin f \rangle = \frac{1J}{2(1-\epsilon^2)^{3/2}a^3} \frac{eh}{p} (P_x Q_y - P_y Q_x) ; \quad (51)$$

By Eq.(50) and Eq.(51), we have

$$\frac{d!^0}{dt} = \frac{p}{nae} \frac{1}{1-\epsilon^2} f [ a_2 \hat{n} ] \cos f + (1 + \frac{r}{p}) [ a_2 \hat{t} ] \sin f g : \quad (52)$$

therefore, by the standard perturbation (Roy (1991); Yi (1993); Liu (1993)), the advance of precession of periastron induced by S-L coupling is given by

$$\frac{d!}{dt} = \frac{d!^0}{dt} - \frac{d}{dt} \cos \frac{LJ}{2} : \quad (53)$$

By putting Eq.(50) and Eq.(51) into Eq.(53), and averaging over one orbital period we have,

$$\langle \frac{d!}{dt} \rangle = \frac{3}{2} \frac{1J}{(1-\epsilon^2)^{3/2}a^3} (P_x Q_y - P_y Q_x) - \frac{d}{dt} \cos \frac{LJ}{2} : \quad (54)$$

Using perturbation equations as in (Roy (1991); Yi (1993); Liu (1993)), and by Eq.(48) and Eq.(54), we have

$$\begin{aligned} \langle \frac{d\$}{dt} \rangle &= \frac{3}{2} \frac{1J}{(1-\epsilon^2)^{3/2}a^3} (P_x Q_y - P_y Q_x) + 2 \frac{d}{dt} \sin^2 \frac{LJ}{2} \\ &= \frac{3}{2} \frac{1J}{(1-\epsilon^2)^{3/2}a^3} (P_x Q_y - P_y Q_x) + O(c^5) : \end{aligned} \quad (55)$$

Eq.(49), Eq.(54) and Eq.(55) indicate that the magnitude of  $d = dt$ , and  $d\$ = dt$  are both  $3L = 2a^3$  (1PN), whereas,  $d! = dt$  is 1.5PN (or zero in 1PN), in the sense that  $d! = dt$  ( $3J = 2a^3$     $3L = 2a^3$ ), as shown in Eq.(54).

$d = dt$  (1PN) of Eq.(48) is equivalent to  $-s$  (1PN) which is given by Wex & Kopeikin (1999). This is because the averaged value of  $d = dt$  depends only on  $a_1$ , the first bracket [] of  $a_{so}$ , as shown in Eq.(34). And both this paper ( $a_{so}$  of Eq.(34)) and that of BO equation ( $a_{so}^0$  of Eq.(35)) give the same  $a_1$ . Thus, different authors give the equivalent value on the averaged  $d = dt$ .

Whereas,  $d! = dt$  (1.5PN) of Eq.(54) and  $-s$  (1PN) given by Wex & Kopeikin (1999) are very different in magnitude, and thus  $d\$ = dt$  predicted by this paper and that of Wex and Kopeikin (1999) are also very different. The difference is due to the fact that  $d! = dt$  and  $d\$ = dt$  given by Eq.(54) and Eq.(55) of this paper are obtained by the  $a_{so}$  of Eq.(34); whereas, the corresponding  $d! = dt$  and  $d\$ = dt$  of Wex and Kopeikin (1999), which is equivalent of replacing  $J$  of Eq.(54) and Eq.(55) by  $S$ , are equivalent to that obtained by the  $a_{so}^0$  of Eq.(35).

And in turn, the difference between  $a_{so}$  and  $a_{so}^0$  is due to the fact that  $a_{so}$  includes the triangle constraints (9 degree of freedom); whereas  $a_{so}^0$  (12 degree of freedom) doesn't. Therefore, a small difference in the equation of motion causes significant discrepancy in the variation of elements,  $d! = dt$  and  $d\$ = dt$ , which in turn leads to very different predictions on observational effects.

5. effects on  $\underline{x}$ ,  $P_b$

Whether the definition of  $J$  is satisfied or not, corresponds to very different magnitude on  $a_{so}$  and in turn corresponds to very different effects on the measurable parameters, such as  $\underline{x}$ ,  $P_b$ , for a observer on the Earth.

The relationship of dynamical longitude of the ascending node,  $\underline{L}$ , dynamical longitude of the periastron,  $\underline{L}$ , and the orbital inclination,  $i$ , can be given (Smarr & Blandford 1976, West & Kopeikin 1999)

$$\cos i = \cos I \cos \underline{LJ} - \sin \underline{LJ} \sin I \cos \underline{L} ; \quad (56)$$

and

$$\begin{aligned} \sin i \sin \underline{L}^{\text{obs}} &= (\cos I \sin \underline{LJ} + \cos \underline{LJ} \sin I \cos \underline{L}) \sin \underline{L} \\ &+ \sin I \sin \underline{L} \cos \underline{L} ; \end{aligned} \quad (57)$$

$$\begin{aligned} \sin i \cos \underline{L}^{\text{obs}} &= (\cos I \sin \underline{LJ} + \cos \underline{LJ} \sin I \cos \underline{L}) \cos \underline{L} \\ &+ \sin I \sin \underline{L} \sin \underline{L} ; \end{aligned} \quad (58)$$

where  $I$  is the misalignment angle between  $J$  and the line of sight. The semi major axis of the pulsar is defined as

$$\underline{x} = \frac{a_p \sin i}{c} : \quad (59)$$

where  $a_p$  is the semi major axis of the pulsar. By Eq.(56), we have,

$$\underline{x}_1 = \frac{a_p \cos i \sin \underline{LJ}}{c} = \underline{x} \sin \underline{LJ} \sin \cot i : \quad (60)$$

The semi major axis of the orbit is  $a = \frac{M}{m_2} a_p$ , and since the L-S coupling induced  $\underline{x}$  is a function of  $\underline{L}$  and  $\underline{L}$ , as shown in the appendix, we have

$$\underline{x}_2 = \frac{a_p \sin i}{c} = \frac{\underline{a}}{a} \underline{x} : \quad (61)$$

Therefore, the L-S coupling induced  $\underline{x}$  is given by

$$\underline{x} = \underline{x}_1 + \underline{x}_2 = \underline{x} \sin \underline{LJ} \sin \cot i + \frac{\underline{a}}{a} \underline{x} : \quad (62)$$

By Eq.(62) we have

$$\underline{x} = \underline{x}_1 - + -\cot + \frac{-\underline{LJ} \cos \underline{LJ}}{\sin \underline{LJ}} + \underline{x} \frac{aa \underline{a}^2}{a^2} + \underline{x}_2 \frac{\underline{a}}{a} : \quad (63)$$

Notice that  $\underline{L}$  and  $\underline{L}$  can be obtained by Eq.(48). Considering  $\underline{LJ} = 1$  and by Eq.(57), Eq.(58), the observational advance of precession of periastron is given (Smarr & Blandford 1976, West & Kopeikin 1999),

$$\underline{L}^{\text{obs}} = \underline{L} + \underline{LJ} \cot i \sin \underline{L} : \quad (64)$$

Therefore, we have

$$\underline{\omega}^{\text{obs}} = \underline{\omega}^+ - \omega_{\text{LJ}} \text{ cotisin} : \quad (65)$$

If  $\underline{\omega}$  and  $\omega$  are caused only by the S-L coupling effect ( $H = H_S$ ), then  $\underline{\omega}$  is given by Eq.(54). If we consider all terms of the Hamiltonian, as given by Eq.(2), then  $\underline{\omega}$  should include the contribution by  $H_{\text{PN}}$ , which causes  $\underline{\omega}^{\text{GR}}$ , the advance of precession of periastron predicted by general relativity. In such case  $\underline{\omega}$  in Eq.(65) is replaced by  $\underline{\omega}^{\text{GR}} + \underline{\omega}$ . Thus Eq.(65) can be written as

$$\underline{\omega}^{\text{obs}} = \underline{\omega}^{\text{GR}} + \underline{\omega}^S : \quad (66)$$

where

$$\underline{\omega}^S = \underline{\omega}^+ - \omega_{\text{LJ}} \text{ cotisin} : \quad (67)$$

Notice that  $\underline{\omega}^S$  is a function of time as shown in Eq.(49), Eq.(54) and Eq.(87), whereas,  $\underline{\omega}^{\text{GR}}$  is a constant as shown in Eq.(8).

For a binary pulsar system with negligibly small eccentricity, the effect of the variation in the advance of periastron,  $\omega$ , is absorbed by the redefinition of the orbital frequency. As discussed by Kopeikin (1996),  $\omega^{\text{obs}} + A_e(u)$  is given

$$\omega^{\text{obs}} + A_e(u) = \omega_0 + \frac{2}{P_b} (t - t_0) ; \quad (68)$$

where  $A_e(u)$  is the true anomaly, related to the eccentric anomaly,  $u$ , by the transcendental equation,  $\omega_0$  is the orbital phase at the initial epoch  $t_0$ .

At the time interval,  $t = (t - t_0)$ , there is a corresponding  $\omega^{\text{obs}}$  which causes a corresponding  $P_b$  at the right hand side of Eq.(68), therefore,  $P_b$  is a function of time. Thus we have

$$\omega^{\text{obs}} + A_e(u) = \frac{2}{P_b} t : \quad (69)$$

Write  $1 = P_b$  in Taylor series, we have

$$\frac{1}{P_b} = \frac{1}{P_b(t_0)} - \frac{P_b(t_0)}{P_b^2(t_0)} \frac{t}{t_0} + \dots \quad (70)$$

Considering  $A_e(u) = 2 \pi t / P_b(t_0)$  and by Eq.(69), Eq.(70) obtains,

$$\underline{\omega}^{\text{obs}} = - \frac{2 P_b}{P_b^2} t : \quad (71)$$

Since  $\underline{\omega}^S$  is a function of time, whereas  $\underline{\omega}^{\text{GR}} = \text{const}$ , then we have  $\omega^{\text{obs}} = \underline{\omega}^S$  by Eq.(66). Assume  $F = \underline{\omega}^S$ , and write it in Taylor series as:  $F = F_0 + F_1 t + \frac{1}{2} F_2 t^2$ , obtains  $F = \underline{\omega}^S - F_1 t - \frac{1}{2} F_2 t^2$ . Therefore,  $\underline{\omega}^{\text{obs}}$  of Eq.(71) becomes  $\underline{\omega}^S = \underline{\omega}^S - F_1 t - \frac{1}{2} F_2 t^2$ , from which Eq.(71) can be written as

$$P_b = \frac{\underline{\omega}^S P_b^2}{2} : \quad (72)$$

By Eq.(72), the derivatives of  $P_b$  can be obtained,

$$P_b = \frac{2P_b^2}{P_b} \quad \frac{P_b^2}{2} \frac{d^3!^S}{dt^3} \quad \frac{P_b^2}{2} \frac{d^3!^S}{dt^3}; \quad (73)$$

$$\frac{d^3P_b}{dt^3} \quad \frac{P_b^2}{2} \frac{d^4!^S}{dt^4}; \quad (74)$$

Under Wex and Kopeikin (1999)'s treatment,  $\underline{!}^{\text{obs}} = \underline{!}^{\text{GR}} = \text{const}$ , then the contribution of S-L coupling to  $P_b$  is negligible, and moreover higher order of derivatives of  $P_b$  are zero, i.e.,  $P_b = 0$ . Therefore, the predictions on the S-L coupling induced effects are very different between Wex and Kopeikin (1999)'s and that of this paper.

## 6. confrontation with observation

The precise timing measurement in some binary pulsars provides a chance to test the two kinds of predictions. The orbital motion causes a delay of  $T = r \cdot \underline{k} = r(t) \sin \underline{i}^{\text{obs}}(t) \sin i(t) = c$  in the pulse arrival time, where  $r$  is the pulsar position vector and  $\underline{k}_0$  is the unit vector of the line of sight. The residual  $T = r \cdot \underline{k} = (r \cdot \underline{k})_K$  of the time delay compared with the Keplerian value is of interest (Lai et al. (1995)). Averaging over one orbit  $r = a$ , and in the case  $\underline{i} = \underline{i}^{\text{obs}}$ , the S-L coupling induced residual is,

$$\begin{aligned} T &= \frac{a}{c} \cos i \frac{di}{dt} t \sin \underline{i}^{\text{obs}} + \frac{a \sin i}{c} t \sin \underline{i}^{\text{obs}} + \frac{a \sin i}{c} \underline{i}^{\text{obs}} t \cos \underline{i}^{\text{obs}} \\ &= \underline{x}_1 t \sin \underline{i}^{\text{obs}} + \frac{\underline{a}}{a} \underline{x}_2 t \sin \underline{i}^{\text{obs}} + \underline{x}^{\text{obs}} t \cos \underline{i}^{\text{obs}}; \end{aligned} \quad (75)$$

By Eq.(83), we have  $\underline{a} = a \quad \underline{J} = \underline{a}^3 \quad \underline{!}^{\text{obs}}$ , therefore, the second and third term at the right hand side of Eq.(75) cannot be distinguished in the current treatment of pulsar timing. In other words, the effect of  $\underline{a}$  can be absorbed by  $\underline{i}^{\text{obs}}$ .

Notice that if  $\underline{a} = 0$  and  $\underline{i}^{\text{obs}} = \underline{i}^{\text{GR}} = \text{const}$ , then  $\underline{i}^{\text{obs}}(t) = \underline{i}_0 + \underline{i}^{\text{GR}} t$ , Eq.(75) reduces to the result of Lai et al. (1995), which is based on BO's orbital precession velocity. These two kinds of residuals (those based on BO's and AK's orbital precession velocities) can give the same order of magnitude values on terms  $\underline{i}^{\text{obs}} t$ , whereas they give very different predictions on the term  $\underline{i}^{\text{obs}} t^2$ . Since the effect caused by  $\underline{i}^{\text{obs}} t^2$  can be absorbed by  $P_b$  as given by Eq.(72), BO and AK's orbital precession velocities actually correspond to very different  $P_b$ , which can be tested by observational data.

### 6.1. PSR J2051-0827

As discussed above, the second term at the right hand side of Eq.(62) can be absorbed by  $\dot{x}_{\text{obs}}$ , therefore  $\dot{x} = \dot{x}_{\text{obs}}$ , and by Eq.(60), we have

$$= \frac{\dot{x}}{x \sin_{\text{LJ}} \sin_0} = \frac{di}{dt} \frac{1}{\sin_{\text{LJ}} \sin_0} : \quad (76)$$

According to optical observations, the system is likely to be moderately inclined with an inclination angle  $i = 40^\circ$  (Stappers et al. (2001)). By the measured results of  $x = 0.045$  s,  $\dot{x} = 23(3) \times 10^{14}$  (Doroshenko et al. (2001)), and by assuming  $\sin_{\text{LJ}} \sin_0 = 2 \times 10^3$ , Eq.(76) can be written in magnitude,

$$= \left( \frac{\dot{x}}{2.3 \times 10^{13}} \right) \left( \frac{x}{0.045} \right)^1 \left( \frac{\tan i}{\tan 40^\circ} \right) \left( \frac{\sin_{\text{LJ}} \sin_0}{2 \times 10^3} \right)^1 = 2 \times 10^9 (\text{s}^1) : \quad (77)$$

Notice that in the following estimation of this section all values are absolute values. By Eq.(54), we can assume  $\dot{x}^s = (\dot{x}_{\text{obs}}^s)^2 = 4 \times 10^{18}$ . Thus by Eq.(72),

$$P_b = \frac{1}{2} \left( \frac{\dot{x}^s}{4 \times 10^{18}} \right) \left( \frac{P_b}{0.099d} \right)^2 = 5 \times 10^{11} (\text{ss}^1) : \quad (78)$$

By Eq.(67), we can estimate  $d^3 \dot{x}^s = dt^3 = 8 \times 10^{27} \text{ s}^3$ , similarly, we can estimate  $d^4 \dot{x}^s = dt^4 = 16 \times 10^{36} \text{ s}^4$ .

Therefore, by Eq.(73) and Eq.(74) we have  $P_b = 9 \times 10^{20} \text{ s}^1$  and  $d^3 P_b = dt^3 = 2 \times 10^{28} \text{ s}^2$ . By Eq.(62) and Eq.(63),  $x = \dot{x} = 2 \times 10^9 \text{ s}^1$ , which is well consistent with observation as shown in Table 3.

Therefore, once  $\dot{x}$  is in agreement with the observation, the corresponding  $\dot{x}^s$  can make the derivatives of  $P_b$  be consistent with observation as shown in Table III. Whereas, the effect derived from West and Kopeikin (1999)'s equation can only be consistent with  $\dot{x}$ , the significant derivatives of  $P_b$  cannot be explained.

### 6.2. PSR J1012+5307

By the measured parameters,  $x = 0.58$  s,  $\dot{x} < 1.4 \times 10^{14}$ ,  $i = 52^\circ$  (Lange et al. (2001)), and by assuming  $\sin_{\text{LJ}} \sin_0 = 1 \times 10^3$ , then  $\dot{x}$  is given,

$$= \left( \frac{\dot{x}}{1.4 \times 10^{14}} \right) \left( \frac{x}{0.58} \right)^1 \left( \frac{\tan i}{\tan 52^\circ} \right) \left( \frac{\sin_{\text{LJ}} \sin_0}{1 \times 10^3} \right)^1 = 3 \times 10^{11} (\text{s}^1) ; \quad (79)$$

similarly  $P_b$  can be obtained,

$$P_b = \frac{1}{2} \left( \frac{\dot{x}^s}{9 \times 10^{22}} \right) \left( \frac{P_b}{0.6d} \right)^2 = 4 \times 10^{13} (\text{ss}^1) : \quad (80)$$

The comparison of observational and predicted variabilities are shown Table 4, which are well consistent.

### 6.3. PSR J1713+ 0747

By the measured parameters,  $x = 32.3 \text{ s}$ ,  $\dot{x} = 5(12) \times 10^{15}$ ,  $i = 70^\circ$  (Camillo et al. (1994)), and by assuming  $\sin_{\text{LJ}} \sin_0 = 1 \times 10^4$ , then in magnitude we have,

$$= \left( \frac{x}{5 \times 10^{15}} \right) \left( \frac{x}{32.3} \right)^1 \left( \frac{\tan i}{\tan 70^\circ} \right) \left( \frac{\sin_{\text{LJ}} \sin_0}{1 \times 10^4} \right)^1 = 4 \times 10^{12} (\text{s}^{-1}) ; \quad (81)$$

similarly we have,

$$P_b = \frac{1}{2} \left( \frac{1 \text{ s}}{16 \times 10^{26}} \right) \left( \frac{P_b}{67.8 \text{ d}} \right)^2 = 1 \times 10^{10} (\text{ss}^{-1}) ; \quad (82)$$

The comparison of observational and predicted variabilities are shown Table 5, which are well consistent. Notice that  $x^{\text{obs}}$  and  $P_b^{\text{obs}}$  measured in these three typical binary pulsars cannot be interpreted by the gravitational radiation induced  $x$  and  $P_b$ , since they are 3 or 4 order of magnitude smaller than those of the observational ones.

### 6.4. Discussion

Therefore, the significant  $P_b^{\text{obs}}$  is a natural result of the S-L coupling effect if the triangle constraint is satisfied on BO's equation of motion. In the case that the triangle constraint is not satisfied (12 degree of freedom) on the BO equation, the contribution of S-L coupling to the advance of precession of periastron relative to the line of sight is insignificant. And in turn the S-L coupling's contribution to  $P_b$  is also insignificant. And since the gravitational radiation induced  $P_b^{\text{GR}}$  is much smaller than that of the measured one,  $P_b^{\text{obs}}$ , thus West and Kopeikin (1999)'s equation cannot explain the significant  $P_b^{\text{obs}}$ .

Applegate & Shaham ((1994)) proposed a model to explain the significant  $P_b^{\text{obs}}$ . Their model assumes a variable quadrupole moment which is due to the cyclic spin-up and spin-down of the outer layers of the companion. In which  $P_b^{\text{obs}}$  of binary pulsars like PSR J2051-0827 can be explained. However the higher derivatives like,  $P_b$ ,  $d^3P_b/dt^3$  of these binary pulsars cannot be well explained by this model. Moreover it is also not easy to explain binary pulsars with much larger orbital period, i.e., PSR J1713+ 0747 ( $P_b = 67.8 \text{ day}$ ); whereas these phenomena can be well explained by S-L coupling induced effect in the case that the triangle constraint is satisfied (9 degree of freedom).

## 7. conclusion

Starting from the same relativistic Hamiltonian, Eq.(3), and precession of spins Eq.(1), one can obtain variabilities by different means, and the results are different significantly in magnitude, as shown in Table 2. The discrepancy is not due to different expression in different coordinate systems. Instead it is due to that the two different expressions are obtained under two different physical conditions, one satisfies the triangle constraint and one violates it. The one that satisfies

the triangle constraint corresponds to 9 degree of freedom for a binary system, whereas, the one that violate it corresponds to 12 degree of freedom. This is similar to calculate the motion of a clock pendulum by two degree of freedom or by one degree of freedom.

The calculation under 12 degree of freedom leads to insignificant parameters i.e.,  $\mathbf{l}^{\text{obs}}$  and  $P_b$ ; whereas, the calculation under 9 degree of freedom leads to significant  $\mathbf{l}^{\text{obs}}$  and  $P_b$ , as shown in Table 2, which can well explain the significant parameters measured on three typical binary pulsars, as shown in Table 3 to Table 5.

I thank T. Huang for help in clarifying the theoretical part of this paper. I thank R. N. M. Anchaster for his help in understanding pulsar timing measurement. I thank T. Lu for useful comments during this work. I thank W. T. Ni and C. M. Xu for useful suggestions in the presentation of this paper. I thank E. K. Hu, A. Rüdiger, K. S. Cheng, N. S. Zhong, and Z. G. Dai for continuous encouragement and help. I also thank Y. Li, Z. X. Yu, C. M. Zhang, L. Zhang, Z. Li, H. Zhang, S. Y. Liu, X. N. Lou, X. S. Wan for useful discussions.

## 8. appendix

By  $\mathbf{S} = a_{\text{so}} \hat{n}$  and  $T = a_{\text{so}} \hat{t}$ ,  $\frac{d}{dt}$  and  $\frac{d^2}{dt^2}$  have been given by Eq.(48), Eq.(49), Eq.(52), and Eq.(54), following the standard procedure for computing perturbations of orbital elements Roy (1991). Similarly, four other elements can be given:

$$\frac{da}{dt} = \frac{p^2}{n^2 (1 - \epsilon^2)} (\mathbf{S} \sin f + \frac{p \mathbf{F}}{r}) ; \quad (83)$$

$$\frac{de}{dt} = \frac{p}{na} \frac{1 - \epsilon^2}{1 - \epsilon^2} [\mathbf{S} \sin f + \mathbf{P} (\cos E + \cos f)] ; \quad (84)$$

$$\langle \frac{de}{dt} \rangle = \frac{1^J e}{(1 - \epsilon^2)^{3/2} a^3} (P_x Q_y - P_y Q_x) ; \quad (85)$$

$$\frac{d_{LJ}}{dt} = \frac{\mathbf{F} r \cos(\mathbf{l} + f)}{na^2 (1 - \epsilon^2)} \frac{1}{\sin_{LJ}} ; \quad (86)$$

$$\begin{aligned} \langle \frac{d_{LJ}}{dt} \rangle = & \frac{3 \cos_{LJ}}{2a^3 (1 - \epsilon^2)^{3/2} \sin_{LJ}} (P_z \cos \mathbf{l} + Q_x \sin \mathbf{l}) [(P_y Q_z - P_z Q_y) (S_{x-1} + S_{2x-2}) \\ & + (P_z Q_x - P_x Q_z) (S_{y-1} + S_{2y-2}) + (P_x Q_y - P_y Q_x) (S_{z-1} + S_{2z-2})] ; \end{aligned} \quad (87)$$

$$\frac{d}{dt} = \frac{e^2}{p^2 (1 - \epsilon^2)} \frac{dS}{dt} + 2 \frac{d}{dt} (1 - \epsilon^2)^{1/2} (\sin^2 \frac{LJ}{2}) \frac{2rS}{na^2} ; \quad (88)$$

where  $\frac{d\$}{dt} = \frac{d!^0}{dt} + 2 \frac{d}{dt} (\sin^2 \frac{LJ}{2})$ .

$$\begin{aligned}
 \langle \frac{d}{dt} \rangle &= \frac{e^2}{1 + \frac{1}{1 - \epsilon^2}} \langle \frac{d\$}{dt} \rangle + 2 \langle \frac{d}{dt} \rangle (1 - \epsilon^2)^{1/2} (\sin^2 \frac{LJ}{2}) \\
 &\quad \frac{1J}{a^3 (1 - \epsilon^2)} (P_x Q_y - P_y Q_x); \tag{89}
 \end{aligned}$$

## REFERENCES

Apostolatos, T. A., Cutler, C., Sussman, J. J., Thorne, K. S., 1994, *Phys. Rev. D*, 49, 6274{6297 .

Applegate, J. H., Shaham, J., 1994, *Astrophys. J.* 436, 312{318 .

Barker, B. M., O'Connell, R. F., 1975, *Phys. Rev. D*, 12, 329{335.

Camilo, F., Foster, R. S., Wolszczan, A., 1994, *Astrophys. J.* 437, L39{L42 .

Damour, T., Schaefer, G., 1988 *IL Nuovo Cimento*, 101B, 127 .

Doroshenko, O., Lohmer, O., Krammer, M., Jessner, A., Wielebinski, R., Lyne, A. G., Lange, Ch., 2001, *Astro-Astrophys.*, 379, 579{588 .

Hamilton, A. J. S., Sarazin, C. L., 1982, *MNRAS* 198, 59{70 .

Kidder, L. E., 1995, *Phys. Rev. D*, 52, 821{847.

Kopeikin, S. M., 1996, *Astrophys. J.* 467, L93{L95.

Lai, D., Bildsten, L., Kaspi, V., 1995, *Astrophys. J.* 452, 819{824 .

Lange, Ch., Camilo, F., Wex, N., Krammer, M., Backer, D. C., Lyne, A. G., 2001, *MNRAS* 326, 274.

Liu, L., 1993, *Method in Celestial Mechanics*, Nanjing University Press

Roy, A. E., 1991, *Orbital Motion*, Adam Hilger

Smarr, L. L., Landford, R. D., 1976, *Astrophys. J.* 207, 574{588.

Stappers, B. W., Van Kerckhove, M. H., Bell, J. F., Kulkami, S. R., 2001, *Astrophys. J.* 548, L183{L186 .

Wex, N., Kopeikin, S. M., 1999, *Astrophys. J.* 514, 388.

Yi, Z. H., 1993, *Essential Celestial Mechanics*, Nanjing University Press

Table 1: Comparison of BO's  $\rightarrow_s$  and AK's  $\rightarrow_0$ 

		BO	AK
1	- equals	$\rightarrow_s \hat{S} \cdot 3\hat{L} \cdot \hat{S} \cdot \hat{L}$	$\frac{J}{2r^3} (4 + \frac{3m_2}{m_1})$
2	L precesses around	instantaneous axis	fixed axis
3	when $J \neq L + S$	$J \neq 0$	$J \neq 0$
4	- obtained by	$L \& A$	$J \& a$
5	degree of freedom	12	9

<sup>a</sup> represents the triangle constraint. The different behaviors, from item 1 to item 4, are determined by item 5 the different degree of freedom of a binary system used by BO and AK in the calculation of the precession of L.

Table 2: Comparison of S-L coupling induced variabilities given by different authors

	A	B	evidence
$-(\rightarrow_s)$ in $J\text{-co}^a$	1PN	1PN <sup>b</sup>	
$!(\rightarrow_s)$ in $J\text{-co}$	1PN	1.5PN	
$!_{\text{obs}}$	$!_{\text{GR}} + 1.5\text{PN}$	$!_{\text{GR}} + 1\text{PN}$	
$P_b$	$P_b^{\text{GR}}$	$P_b^{\text{GR}}$	$\frac{!^s P_b^2}{2}$
<sup>d</sup>	No	Yes	$P_b^{\text{obs}} j$

A : given by BO and Wex & Kopeikin (1999), B :  $-(\rightarrow)$  in one spin case is given by Apostolatos et al. (1994) and Kidder (1995), others are given by this paper. <sup>a</sup> J-co represents J-coordinate system, <sup>b</sup> Apostolatos et al. (1994) and Kidder (1995), <sup>c</sup> references (2001; 2001? ; 2001; 1994). <sup>d</sup> represents the triangle constraint. Notice that except for  $-(\rightarrow)$ , all other parameters predicted by the two models are different.

Table 3: Measured parameters compared with the geodetic precession induced ones in PSR J2051-0827

observation	this paper
$x^{\text{obs}}$	$23(3) \cdot 10^4$
$(x=x)$ <sup>obs</sup>	$3.0 \cdot 10^8 \text{ s}^{-1}$
$P_b^{\text{obs}} =$	$15.5(8) \cdot 10^{12}$
$P_b^{\text{obs}} = 2.1(3) \cdot 10^{20} \text{ s}^{-1}$	$\dot{P}_b j = \frac{!^s P_b^2}{2} j \cdot 5 \cdot 10^{11}$
$\frac{d^3 P_b^{\text{obs}}}{dt^3} = 3.6(6) \cdot 10^{28} \text{ s}^{-2}$	$\ddot{P}_b j = \frac{P_b^2 d^3 !^s}{dt^3} j \cdot 9 \cdot 10^{20} \text{ s}^{-1}$
	$\dddot{P}_b j = \frac{P_b^2 d^4 !^s}{dt^4} j \cdot 2 \cdot 10^{28} \text{ s}^{-2}$

Table 4: Measured parameters compared with the geodetic precession induced ones in PSR J1012+ 5307

observation	this paper
$\dot{x}_j^{\text{obs}} < 1.4 \quad 10^{14}$	$\dot{x} = \dot{x}^{\text{obs}}$
$P_b^{\text{obs}} = 1 \quad 10^{13}$	$\dot{P}_b j = \frac{1}{2} \frac{s P_b^2}{j} \quad 4 \quad 10^{13}$

Table 5: Measured parameters compared with the geodetic precession induced ones in PSR J1713+ 0747

observation	this paper
$\dot{x}_j^{\text{obs}} = 5(12) \quad 10^{15}$	$\dot{x} = \dot{x}^{\text{obs}}$
$P_b^{\text{obs}} = 1(29) \quad 10^{11}$	$\dot{P}_b j = \frac{1}{2} \frac{s P_b^2}{j} \quad 1 \quad 10^{10}$

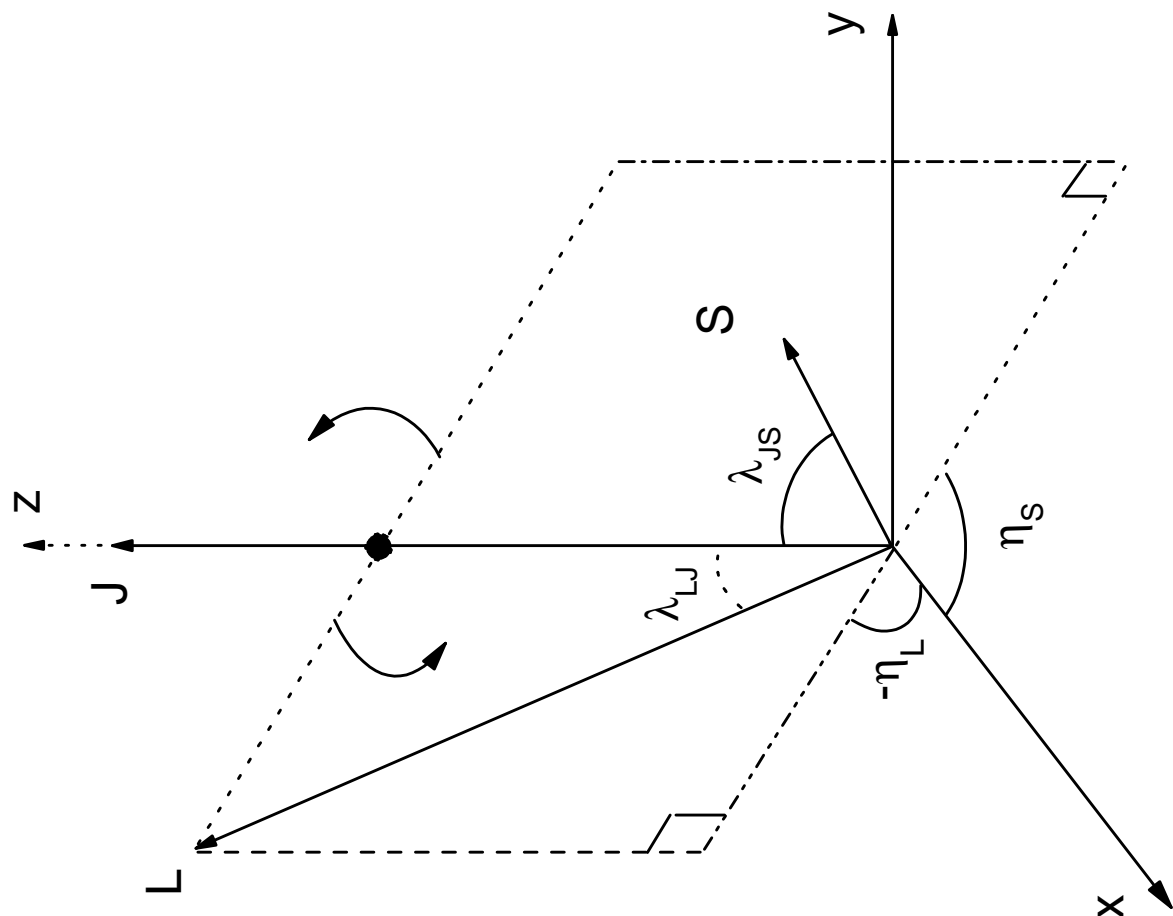


Fig. 1. In 1PN, the scenario of motion of a binary pulsar system can be described as the rotation of the plane determined by  $L$ ,  $S$  around the fixed axis,  $J$ .  $\eta_L$  and  $\eta_S$  are precession phases of  $L$  and  $S$  in the  $J$ -coordinate system respectively.

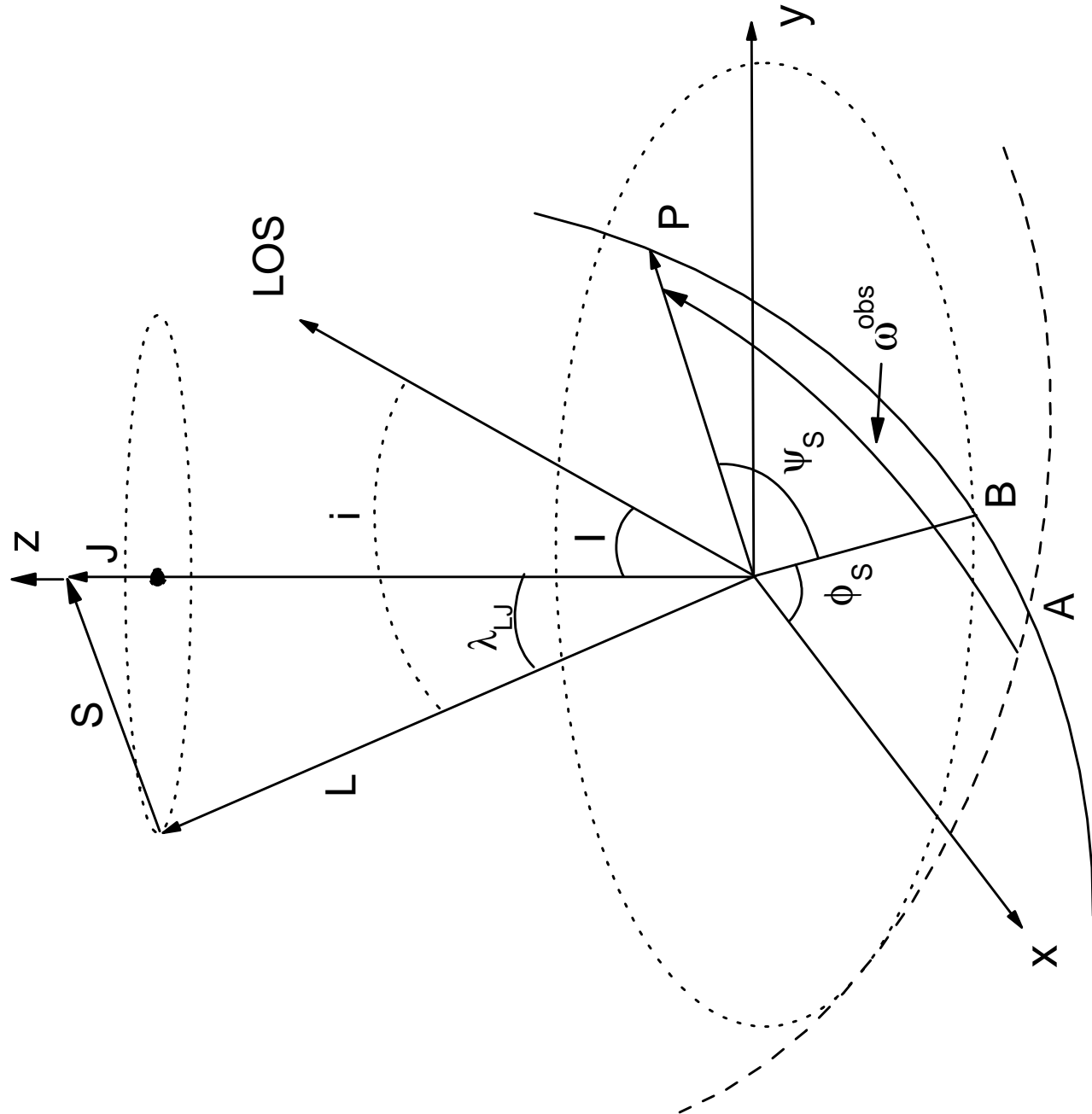


Fig. 2.1 Binary geometry and definitions of angles. The invariable plane (x-y), as represented by the dotted ellipse, is perpendicular to the total angular momentum,  $J$ . The inclination of the orbital plane with respect to the invariable plane is  $\lambda_{LJ}$ , which is also the precession cone angle of

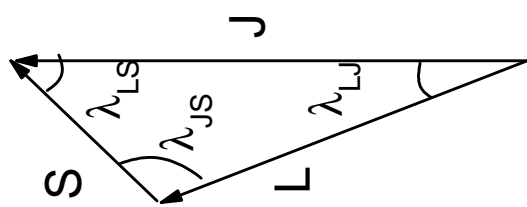
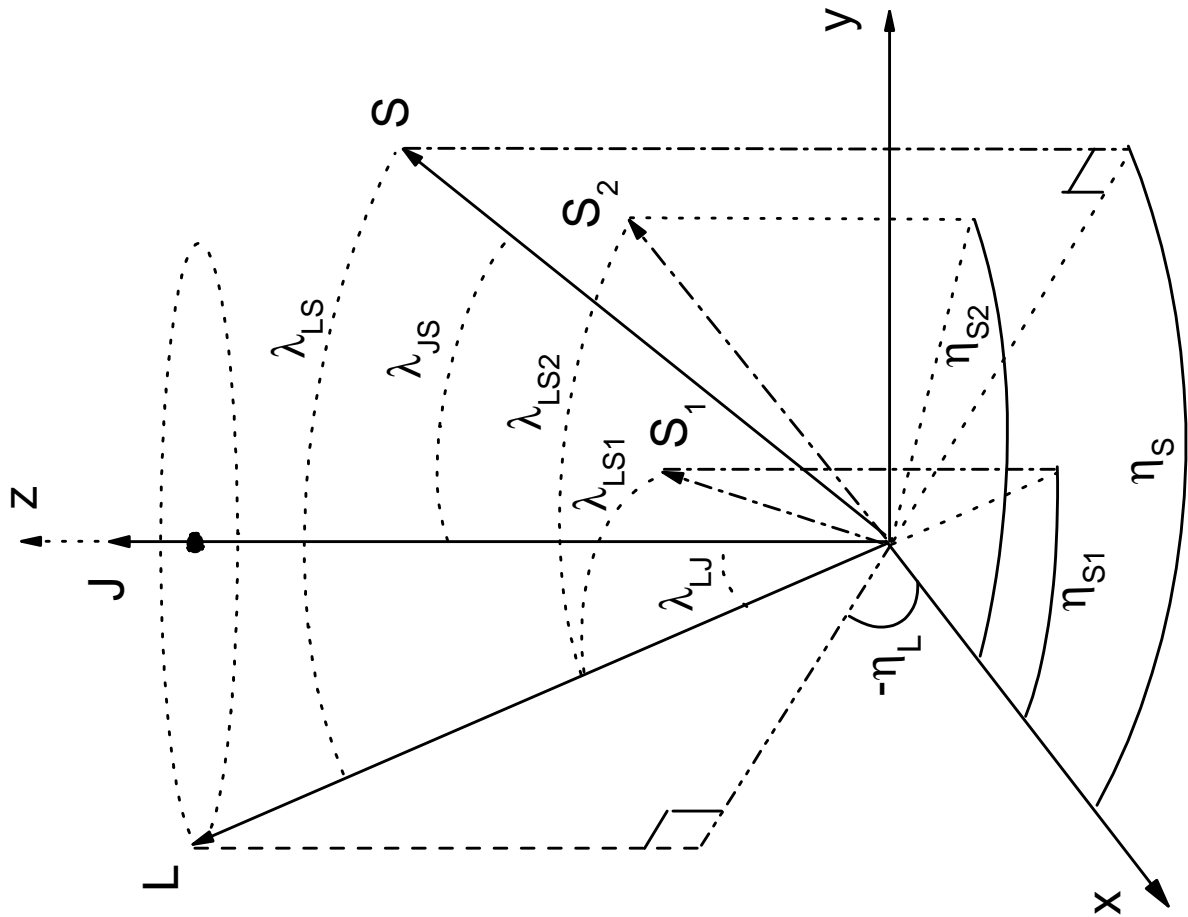


Fig. 3. | Angles and orientation conventions relating vectors  $S$ ,  $L$  and  $J$  to the coordinate system .  $x$ - $y$  is the invariance plane,  $s_1$ ,  $s_2$ ,  $s$  and  $_{_L}$  are precession phases of  $S_1$ ,  $S_2$ ,  $S$  and  $L$ , respectively.